PREPRINT

PERTANIKA JOURNALS

SCIENCE & TECHNOLOGY

Journal homepage: http://www.pertanika.upm.edu.my/

Examining the Impact of Battery Properties and Energy Storage Connectivity for Electric Vehicle Charging Performance

Muhammad Izzul Mawardi[1], Nik Hakimi Nik Ali[1,2,*], Muhamad Nabil Hidayat[1,2], Ezmin Abdullah[1,2], Muhammad Umair[1,2], Ahmad Sukri Ahmad[3] and Muzakkir Mohammad Zainol[4]

[1]*School of Electrical Engineering, College of Engineering, Universiti Teknologi MARA, 40450 Shah Alam, Selangor, Malaysia*

[2]*Battery Energy Storage Technology Laboratory (BEST), College of Engineering, Universiti Teknologi MARA, 40450 Shah Alam, Selangor, Malaysia*

[3]*Petronas Research Sdn Bhd, Bangi Government, and Private Training Centre Area, 43000 Bandar Baru Bangi, Selangor, Malaysia*

[4]*School of Chemical Engineering, College of Engineering, Universiti Teknologi MARA, 40450 Shah Alam, Selangor, Malaysia*

ABSTRACT

Carbon emissions from fossil fuels significantly contribute to global warming. To mitigate these emissions, Electric Vehicles (EVs) and renewable energy stored in Energy Storage Systems (ESS) have been introduced to achieve net-zero carbon emissions. Various types of batteries, including Lithium-Ion (Li-Ion), Lead Acid (Pb-Acid), and Nickel Cadmium (NiCd), are used in EVs and ESS to meet the increasing demand. This article examines the effect of different battery profiles on the performance of batteries in ESS. The paper presents a simulation study of an EV charging system using MATLAB, incorporating a 600 V ESS battery with a 100 Ah capacity and an EV battery rated at 400 V and 50 Ah. The study explores the charging and discharging performance of Li-Ion, Pb-Acid, and NiCd batteries and investigates the impact of different battery connection arrangements and aging factors on battery performance. According to the findings, the state of charge (SOC), voltage, and current significantly influence battery charging and discharging performance. The results suggest that Li-Ion batteries with series-parallel connections outperform others, maintaining approximately 49.93% SOC with a minimal 0.07% drop after 10 seconds. Furthermore, aging batteries show a faster SOC decline, with Li-Ion batteries demonstrating the most stable performance across metrics. The

ARTICLE INFO

Article history:
Received: 31 July 2024
Accepted: 16 January 2025
Published: 26 March 2025

DOI: https://doi.org/10.47836/pjst.33.3.06

E-mail addresses:
Muhammadizzulizz972@gmail.com (Muhammad Izzul Mawardi)
hakimiali@uitm.edu.my (Nik Hakimi Nik Ali)
mnabil@uitm.edu.my (Muhamad Nabil Hidayat)
ezmin@uitm.edu.my (Ezmin Abdullah)
drumair@uitm.edu.my (Muhammad Umair)
ahmadsukri.ahmad@petronas.com (Ahmad Sukri Ahmad)
muzakkir@uitm.edu.my (Muzakkir Mohammad Zainol)
*Corresponding author

e-ISSN: 2231-8526

research highlights that series-parallel Li-Ion configurations best support EV charging applications due to their efficiency and durability.

Keywords: Battery properties, electric vehicle, energy storage system

INTRODUCTION

Vehicles powered by gasoline play a significant role in emitting carbon, adversely impacting the environment. In 2015, such vehicles were responsible for 40% of the world's carbon dioxide emissions, projected to double by 2050 (Al-Hanahi et al., 2022; Jeon et al.,2021). Carbon emissions significantly contribute to global warming and climate change, resulting in extreme weather events. To achieve zero carbon emissions, electric vehicles (EVs) present a viable alternative to reduce the number of gasoline-fueled vehicles on the road (Umair et al., 2024; Said et al., 2015; Said, 2021; Said & Elloumi, 2022). EVs can operate with the same potential as gasoline-fueled vehicles while benefiting the environment by producing no carbon emissions. EVs and energy storage systems (ESS) rely on batteries for power by utilizing various types of batteries such as Lithium-Ion (Li-Ion), Lead-Acid (Pb-Acid), and Nickel-Cadmium (NiCd). However, several battery parameters must be considered when designing and modeling ESS and EVs. The parameters used to assess battery performance in ESS and EVs include state of charge (SOC), depth of discharge (DOD), state of discharge (SOD), battery efficiency, temperature, and degradation (Rosewater et al., 2019; Schommer et al., 2024). It is important to select the appropriate battery type to optimize system performance.

One major issue is the lack of an adequate model to analyze EV charging performance, which hinders the development of public charging infrastructure (Alghamdi et al., 2020; Arfeen et al., 2010). To increase the widespread use of EVs, a robust charging performance infrastructure must be established to support the growing demand (Al-Hanahi et al., 2022; Samadani et al., 2012). Different battery types affect the performance of ESS and EVs due to their unique characteristics. Each battery type exhibits varying performance and efficiency in charging and discharging, necessitating in-depth analysis and simulation to understand these differences (Gong et al., 2015). Li-Ion batteries exhibit higher energy density, longer cycle life, and lower self-discharge rates than Pb-Acid batteries (Miao et al., 2019; Talele et al., 2024; Bais et al., 2024; Jiang et al., 2024). Li-Ion batteries also have a relatively flat discharge voltage curve, offer stable output over a wide SOC range, and are lightweight (Hannan et al., 2018; Tran et al., 2021). While less expensive, Pb-Acid batteries are considered safer and have a flatter discharge voltage curve, making them suitable for cost-sensitive applications NiCd batteries, known for their temperature tolerance and reliability, fall between Pb-Acid and Li-Ion batteries in terms of energy density and weight. NiCd batteries can tolerate overcharging and deep discharging better but may be

susceptible to memory effects. The choice of battery technology in ESS and EVs depends on cost, cycle life, weight, safety, and specific application requirements.

The connection arrangement of the battery, whether in series, parallel or a combination series-parallel, also significantly influences battery charging and discharging performance (Gong et al., 2015). Additionally, charging and discharging can cause battery degradation, reducing cycle life and capacity due to the heat generated during these processes. This highlights the need for a comprehensive exploration of EV charging performance, considering battery connection arrangements and aging profiles (Timilsina et al., 2023; Lehtola & Zahedi, 2021). The connection arrangement of batteries in an ESS profoundly influences charging and discharging dynamics, whether in series, parallel, or combination configurations (Cho et al., 2019). In series connections, batteries are linked end-to-end, increasing the total voltage while maintaining the same overall capacity. In parallel connections, where batteries are connected with corresponding terminals, the total voltage is maintained while the overall capacity is improved.

The series-parallel combination allows for achieving specific voltage, capacity, and current requirements. During charging, series and parallel configurations impact current and voltage distribution. The arrangement determines the overall voltage and current handling capabilities during discharging. Careful consideration of these connections is essential, including balancing individual batteries to prevent over-charging, over-discharging, and uneven current distribution. This ultimately influences the performance and lifespan of the ESS and EV (Cho et al., 2019). The aging factor in battery systems refers to the gradual degradation of a battery's performance over time, influenced by cycle life, calendar life, temperature, DOD, and charging practices (Li et al., 2023). This aging process significantly affects the SOC and SOD of the battery. As the battery ages, its capacity diminishes, reducing the achievable SOC during charging and the available energy during discharge. Additionally, changes in voltage characteristics and increased internal resistance further complicate accurate SOC estimation (Kumar et al., 2023; Said, 2021).

The primary objective of this study is to develop and design a model for an ESS charging system using MATLAB. The study also aims to simulate and analyze the effect of three different battery types, Li-Ion, Pb-Acid, and NiCd, on charging and discharging performance. The research focuses on analyzing EV charging performance as influenced by the type of battery, connection arrangement, and aging factor of ESS. This study is particularly important due to the increasing demand for efficient and sustainable ESS in EVs. As EV adoption continues to grow, understanding the variation of battery performance and longevity is critical for optimizing charging systems. Previous research has primarily focused on individual aspects of battery performance or specific battery types without considering a holistic approach that simultaneously encompasses different battery chemistries, their arrangement, and aging effects.

Contribution

The novelty of this paper lies in its comprehensive approach to studying the interplay between various battery types and configurations within an ESS charging system through a bidirectional DC-DC (BDC) converter to charge EV batteries. By employing MATLAB for simulation, the research provides detailed insights into how each variable affects overall performance. This study addresses a significant research gap by integrating multiple factors that influence EV charging efficiency and battery life, which have often been studied in isolation. The findings from this research contribute new knowledge to the literature, offering a more complete understanding of ESS dynamics with battery types, connections arrangement, and aging factors study and paving the way for advancements in EV technology and sustainable transportation solutions.

METHODOLOGY

Overall System

Figure 1 shows a complete layout diagram of the proposed AC-DC EV Charging Station with ESS integration. As per Nissan Leaf EV specifications, a 400 V with 40 kW power for each EV is considered for the charging station (Sundararajan & Iqbal, 2021). In this paper, ESS will help balance the supply and demand of energy for EV chargers using a bidirectional DC-DC converter. The system simulation is performed using MATLAB. Still, this study only focused on one type of mode, which is discharging ESS to EV Battery

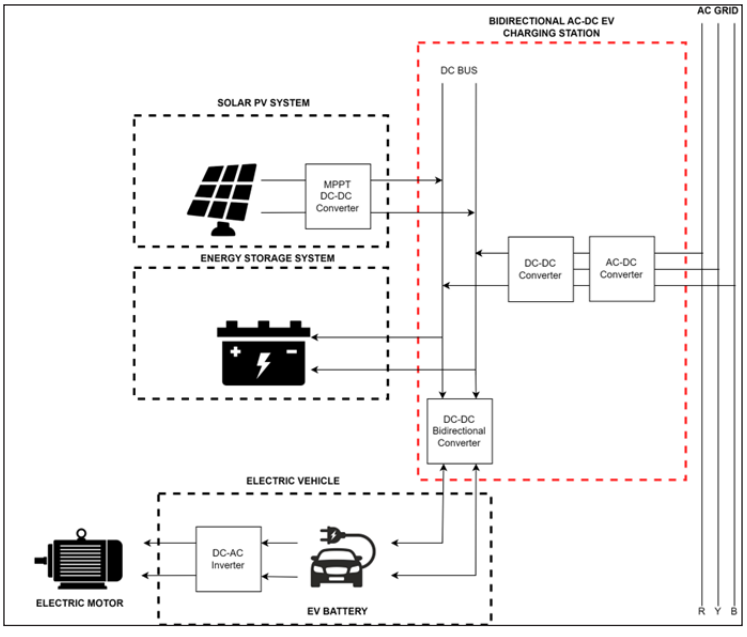

Figure 1. Layout diagram of proposed AC-DC EV Charging Station with ESS integration

Integration, because this mode is crucial for optimizing the efficiency and reliability of EV charging stations. By focusing on discharging, the study aims to ensure that the energy stored in the ESS can be effectively and efficiently transferred to the EV batteries, a common and essential operation in practical scenarios. The ESS battery type was Li-Ion, Pb-Acid, or NiCd. The ESS was connected to a bidirectional converter connecting to the EV battery to allow bidirectional charging and discharging to operate in two directions.

Flowchart of System

The flowchart shows the data collection based on established standards in the simulation process. Parameters were defined, and the circuit design was developed accordingly. Subsequently, system testing was conducted to validate the design. A decision point was introduced to address potential errors. If an error was detected, the flowchart directed the process to troubleshooting steps. In the absence of errors, the simulation proceeded with different cases. Three cases are defined in this study: Case 1, Case 2, and Case 3.

Case 1 utilized Li-Ion, Pb-Acid, and NiCd with identical battery parameters but varying discharging characteristics based on their specific chemistry and discharge curves. Every type of battery will produce its battery properties.

Case 2 involved testing different connection arrangements of batteries. Series, parallel, and series-parallel connections were tested in the simulation, using six batteries connected in series and another set of six batteries connected in parallel. A combination connection arrangement with twelve batteries connected in a series-parallel configuration was included.

Case 3 explored the aging factor of the batteries. The performance of aged batteries was compared with non-aged batteries for a comprehensive assessment of performance changes over time.

Finally, the simulation concluded with an in-depth analysis of the results. This structured approach facilitated a systematic and comprehensive simulation process, allowing for efficient troubleshooting and the exploration of various scenarios in the simulation environment. The flowchart is shown in Figure 2.

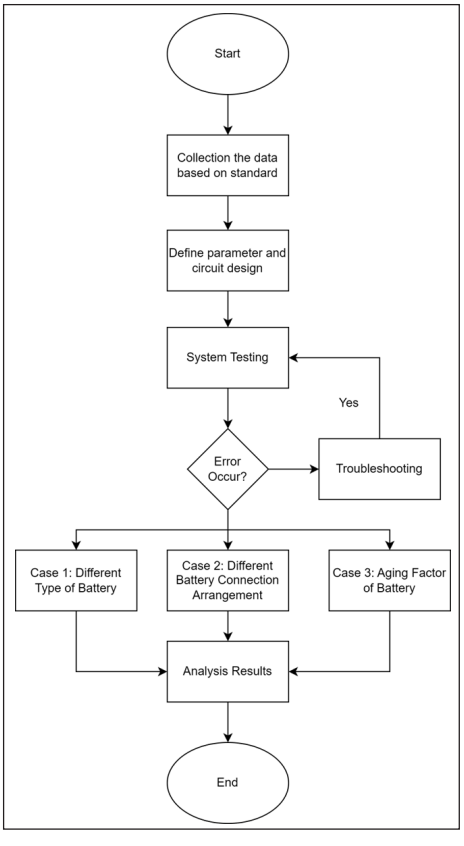

Figure 2. Flowchart of system

System Parameters

Table 1 represents the battery parameters of ESS and EV. A battery model was developed with three types of batteries: Li-Ion, Pb-Acid, and NiCd, to integrate with the ESS, while the EV only uses the Li-Ion type. The model ESS consists of one battery bank with 600 V 100 Ah while the EV battery 400 V 50 Ah is connected in series. The battery model includes parameters such as types of battery, rated capacity, nominal voltage, initial SOC, rated power, and connection. SOC indicates the current charge level of a battery as a percentage of its total capacity. In simple terms, SOC represents how much energy is currently stored in the battery relative to its full capacity (Singh et al., 2023). SOC expression is shown in Equation 1. In battery configuration, there are two processes which are charging and discharging. The expression of charging and discharging expression is shown in Equations 2 and 3.

Table 1
Battery parameters of ESS and EV

Performance Characteristics	**Energy Storage System (ESS) Battery**	**Electric Vehicle (EV) Battery**
Types of Battery	Lead acid, Lithium-ion, and Nickel Cadmium	Lithium-ion
Rated Capacity (Ah)	100	50
Nominal Voltage (V)	600	400
Initial State of Charge (%)	50	50
Rated Power (kWh)	60	20
Connection	series, parallel, series-parallel	series
Aging effect	Aging effect (50 cycles) Without the Aging effect (zero cycle)	Not applicable

$$\text{SOC}\ (\%) = \frac{\text{Capacity Remaining(Ah)}}{\text{Total Capacity}\ \ (\text{Ah})} \quad [1]$$

$$\text{Charging Time (In Hours)} = \frac{\text{Battery Capacity (Ah)}}{\text{Charging Current (A)}} \quad [2]$$

$$\text{Discharging Time (In Hours)} = \frac{\text{Battery Capacity (Ah)}}{\text{Drawing Current (A)}} \quad [3]$$

Converter Circuit and Battery Connection

Figure 3 shows the ESS battery model with an integrating buck-boost BDC to charge the EV battery. The theoretical equation for the buck-boost bidirectional converter is presented below:

The equations describe the relationship between input and output power. Equation 4 shows that input power (Pin) is the product of input voltage (V_{in}) and input current (I_{in}). Equation 5 defines output power ($Pout$) as the product of output voltage (V_{out}) and output current (I_{out}). Equation 6 expresses output power in terms of output voltage squared divided ($V_{out}{}^2$)by load resistance (R).

$$Pin = V_{in} I_{in} \quad [4]$$

$$Pout = V_{out} I_{out} \quad [5]$$

$$Pout = \frac{V_{out}{}^2}{R} \quad [6]$$

Equation 7 defines the duty cycle (D) of a converter as the ratio of the absolute value of the output voltage $|V_{out}|$ to the sum of the input voltage (V_{in}) and the absolute output voltage. The duty cycle determines the proportion of time the switch is on during each cycle, affecting the overall voltage regulation and power transfer efficiency of the converter.

$$D = \frac{|V_{out}|}{V_{in} + |V_{out}|} \quad [7]$$

Equation 8 represents the inductor current (I_L) in a converter, calculated as the product of the input voltage V_{in} and the duty cycle D, divided by the resistance R and the square $(1 - D)$. This equation helps determine the current flowing through the inductor, which is critical for analyzing the converter's operation and performance, particularly in managing energy storage and power delivery.

$$I_L = \frac{V_i D}{R(1 - D)^2} \quad [8]$$

Equations 9 and 10 describe the maximum (I_{max}) and minimum inductor currents (I_{min}) in a converter, where (V_{in}) is the input voltage, (D) in duty cycle, (R) is the load resistance, (T) is switching time, and (L) is inductor.

$$I_{max} = = \frac{V_{in}D}{R(1-D)^2} + \frac{V_{in}DT}{2L} \quad [9]$$

$$I_{min} = = \frac{V_{in}D}{R(1-D)^2} - \frac{V_{in}DT}{2L} \quad [10]$$

Equation 11 calculates the minimum inductance (L_{min}) necessary for proper operation of a converter, given ($\frac{(1-D)^2R}{2f_s}$) where (D) is the duty cycle, (R) is the resistance, and (f_s) is the switching frequency. This equation helps ensure that the inductor is sized correctly to maintain circuit stability and minimize current ripple.

$$L_{min} = \frac{(1-D)^2R}{2f_s} \quad [11]$$

Equation 12 calculates the capacitance (C) needed in a converter circuit, given by ($\frac{D}{Rrf_s}$) where (D) is the duty cycle, (R) is the load resistance,(r) is a ripple voltage, and (f_s)is the switching frequency. This equation helps determine the appropriate capacitor value to ensure stable voltage regulation and minimize voltage ripple in the circuit.

$$C = \frac{D}{Rrf_s} \quad [12]$$

However, this simulation focuses only on the battery part of ESS by considering different battery types, connections, and aging factors. The Li-Ion batteries are connected in three ways: series connection, parallel connection, and series-parallel connection, as shown in Figures 4, 5, and 6. The voltage input to the ESS is set at 600 V. The function of the buck-boost bidirectional converter is to adjust the directional flow of charging and discharging with the current stability to the EV battery from ESS by using the proportional-integral (PI) Controller algorithm. The connection arrangement of the battery was compared between series, parallel, and series-parallel configurations. Finally, the battery aging factor was applied to compare with a non-aging battery only for Li-Ion battery in MATLAB because Li-Ion batteries exhibit more complex degradation mechanisms compared to Pb-Acid and NiCd batteries and limitations on MATLAB block. In this simulation, the battery is cycled 50 times to show the effect of aging and compare it with a battery with a zero life cycle. A new battery means zero life cycle. A new battery that has not undergone any charge or discharge cycles. This battery is used as a baseline to compare the effects

of aging. A battery that has been cycled 50 times to simulate aging. This battery is used to study the impact of 50 charge or discharge cycles on its performance. All these factors were observed and analyzed, including the battery's SOC, voltage, and current performance (Singh et al., 2023).

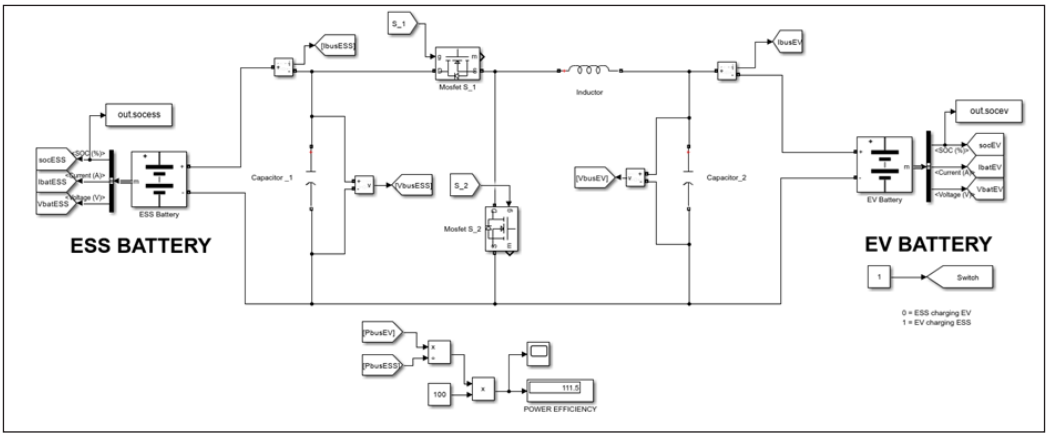

Figure 3. The circuit design for different types of batteries and the aging factor of ESS and EV

In a series connection, the batteries are connected end-to-end, positive to negative, to increase the overall voltage while keeping the same capacity (Gong et al., 2015). The expressions for total voltage and total capacity are shown in Equations 13 and 14.

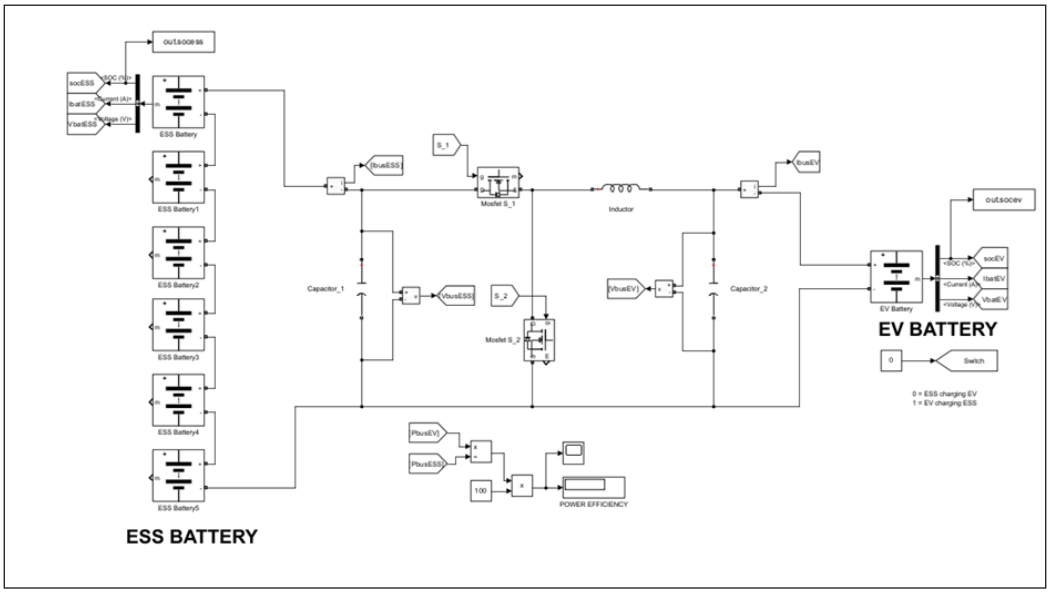

Figure 4. The circuit design of the system for series connection battery

$$\text{Voltage}_{\text{total}} = \text{V}_1 + \text{V}_2 + \text{V}_3 + \text{V}_\text{n} \quad [13]$$

$$\text{Capacity}_{\text{total}} = \text{Capacity}_1 = \text{Capacity}_2 = \text{Capacity}_3 = \text{Capacity}_\text{n} \quad [14]$$

In a parallel connection, the batteries are connected positive to positive and negative to negative to increase the overall capacity while keeping the voltage the same (Gong et al., 2015). The expression of total voltage and total capacity is shown in Equations 15 and 16.

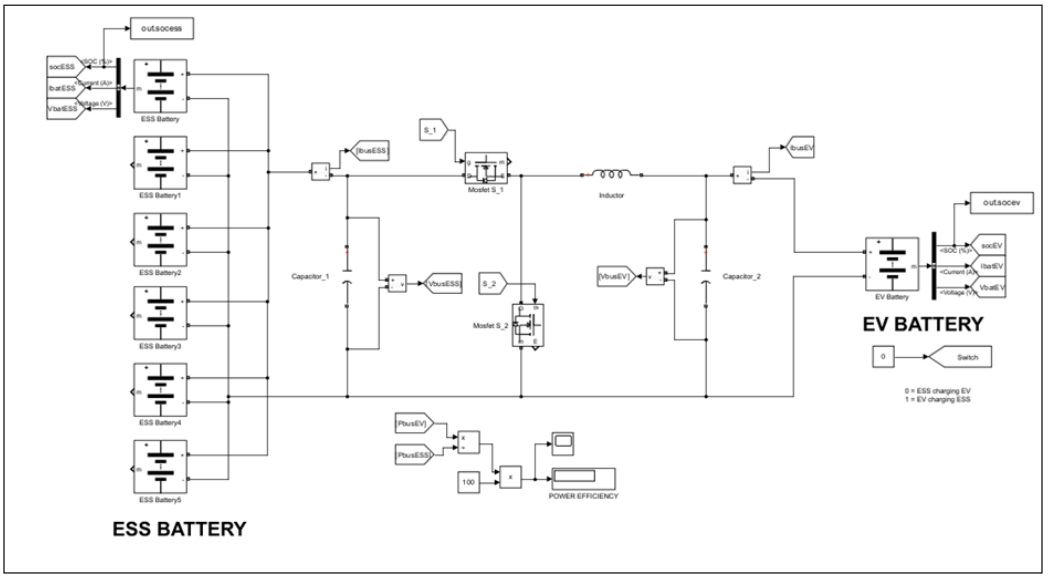

Figure 5. The circuit design of the system for parallel connection battery

$$\text{Vtotal} = \text{V}_1 = \text{V}_2 = \text{V}_3 = \text{V}_\text{n} \quad [15]$$

$$\text{Capacity}_{\text{total}} = \text{Capacity}_1 + \text{Capacity}_2 + \text{Capacity}_3 + \text{Capacity}_\text{n} \quad [16]$$

In a series-parallel connection, the batteries are connected, with some in series and others in parallel. In the series portion, batteries are connected positive to negative, increasing the overall voltage while keeping the same capacity. In the parallel portion, batteries are connected positive to positive and negative to negative, increasing the overall capacity while maintaining the same voltage (Gong et al., 2015). The expressions for total voltage and total capacity are shown in Equations 17 and 18. where n_s is the number of batteries in a series, V is the voltage of a single battery, and n_P is the number of parallel groups, and C is the capacity of a single battery.

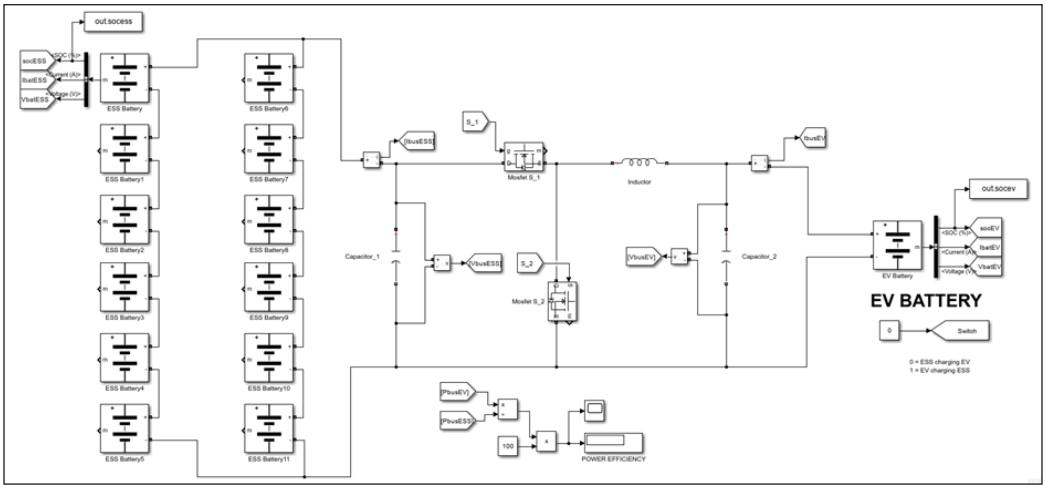

Figure 6. The circuit design of the system for series-parallel connection battery

$$\text{Vtotal} = \text{n}_\text{s} \times \text{V} \quad [17]$$

$$\text{Capacity}_{\text{total}} = \text{n}_\text{p} \times \text{C} \quad [18]$$

PI Controller Algorithm

Figures 7 and 8 present the charging and discharging control algorithms for the buck-boost bidirectional converter to integrate ESS into EV operation. A proportional-integral (PI)-based Pulse width Modulation (PWM) generator is implemented for controlling the bidirectional battery charger circuit using a buck-boost converter with constant-current (CC) 100 A and constant-voltage (CV) 400 V for the EV battery. The comparator compares the reference current and actual current, the output of the comparator generator error signal. The EV battery charges while the ESS battery discharges simultaneously during the buck operation. The converter's input voltage is the DC-link voltage $VbatESS$ generated by the ESS battery, and the output of the converter is the battery voltage $VbatEV$. The control algorithm in Figure 7 regulates the charging process by controlling the two IGBT switches (S_1 and S_2). Initially, the DC-link voltage $VbatESS$ energizes both the inductor and the EV battery. Once the inductor is fully energized, the battery is charged solely by the energy stored in the inductor. The algorithm compares the measured $VbatEV$ with the desired EV battery voltage. The PI voltage controller then minimizes and eliminates the errors to ensure they are equal until the EV battery reaches 100% SOC.

In the boost operation, the control algorithm in Figure 8 regulates the discharging of the EV battery and the charging of the ESS battery simultaneously. The converter's input voltage is the DC-link voltage $VbatEV$ generated by the EV battery, and the output of the converter is the battery voltage $VbatESS$. The control algorithm manages the discharging

process by controlling the two MOSFET switches (S_1 and S_2). Initially, the DC-link voltage $VbatEV$ energizes the inductor and the ESS battery. Once the inductor is fully energized, the ESS battery is charged solely by the energy stored in the inductor. The algorithm compares the measured $VbatESS$ with the desired ESS battery voltage. Figure 9 shows the operation switch of the BDC to change between two modes: Buck mode (charging the EV by discharging the ESS) and Boost mode (discharging the EV by charging the ESS). After the mode operation is selected, the battery current reference $Ibat\_ref$ sends a signal to the PI current controller, as shown in Figure 10, to control the PWM of the two MOSFETs.

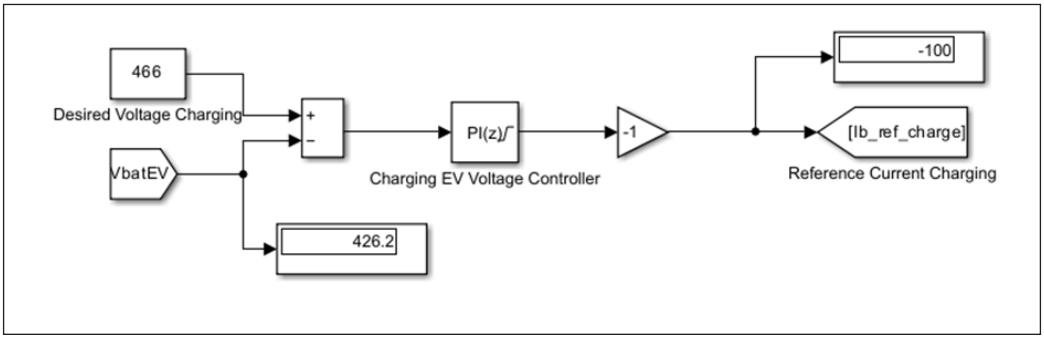

Figure 7. Reference current for charging EV operation

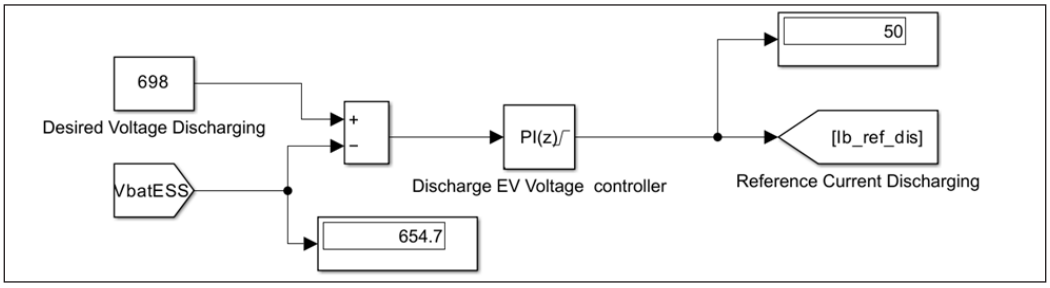

Figure 8. Reference current for discharging EV operation

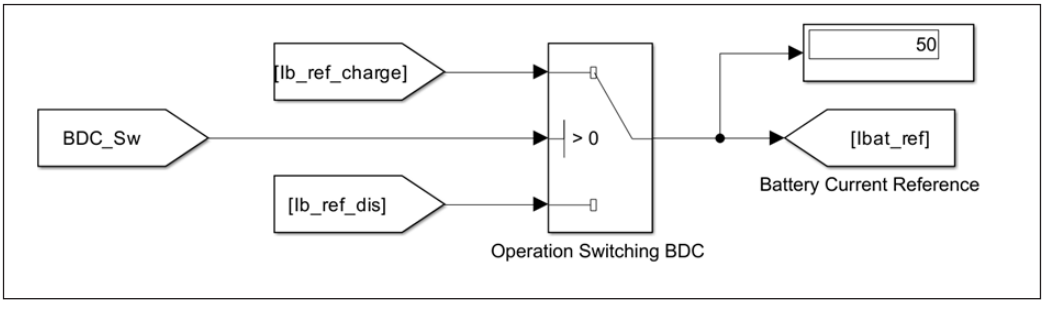

Figure 9. Operation switching of BDC

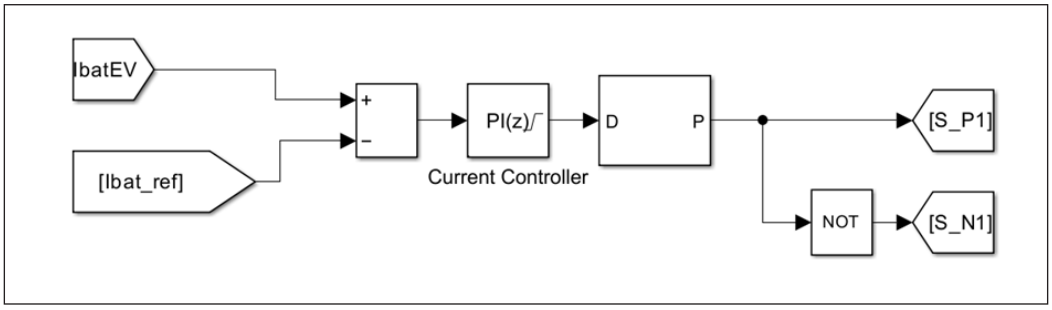

Figure 10. PI Controller used for PWM (Pulse Width Modulation) control

SIMULATION RESULTS

Case 1 – Battery Types

Figure 11 illustrates the SOC, voltage, and current of three different types of batteries: Pb-Acid, Li-Ion, and NiCd over time. All three batteries show a decrease in SOC, as expected during discharge. The Pb-Acid battery (blue line) has the steepest slope, indicating the fastest discharge rate. In contrast, the Li-Ion battery (red line) has a moderate slope, showing a slower discharge rate compared to Pb-Acid but faster than NiCd. The NiCd battery (yellow line) has the least steep slope, indicating the slowest discharge rate. Initially, time, t=0, all three batteries start with a SOC of 50%. By t=10, the SOC of the Pb-Acid battery drops to about 49.75%, the Li-Ion battery to around 49.8%, and the NiCd battery maintains the highest SOC at about 49.85%. It is observed that the SOC of Pb-Acid, Li-Ion, and NiCd dropped by 0.5%, 0.4%, and 0.3% in 10 seconds, respectively. The Li-Ion battery has the highest nominal voltage at around 640 V, followed by NiCd at approximately 620 V and Pb-Acid at about 560 V, showing minimal fluctuations over time. It was found that the nominal voltage of Li-Ion was around 14.29% higher than the nominal voltage of Pb-Acid batteries for a defined period t=10. The current readings reveal that Pb-Acid delivers a higher and more stable current, around 80 A, indicating a more constant load, while the Li-Ion and NiCd batteries, both around 75 A, show more fluctuations, reflecting dynamic responses to load changes. This trend highlights that Pb-Acid batteries, with higher internal resistance and lower efficiency, discharge more quickly. In contrast, Li-Ion batteries, with higher energy density and better efficiency, discharge more slowly. Despite having lower energy density than Li-Ion, NiCd batteries are robust and have a lower self-discharge rate, resulting in the slowest SOC decrease among the three types. Overall, the observed current and voltage levels align with the characteristics of these battery types, with Pb-Acid typically providing higher discharge currents compared to Li-Ion and NiCd.

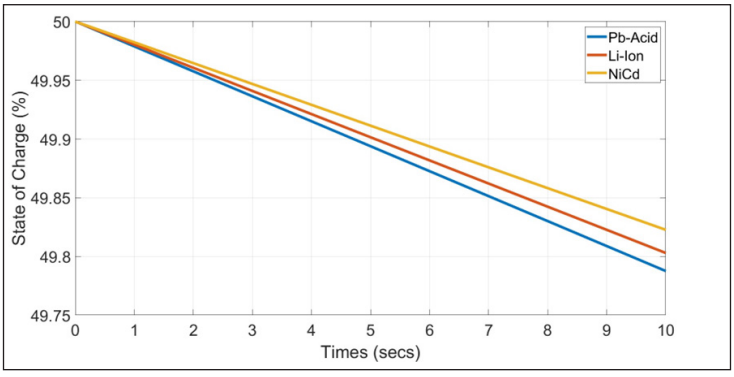

(a)

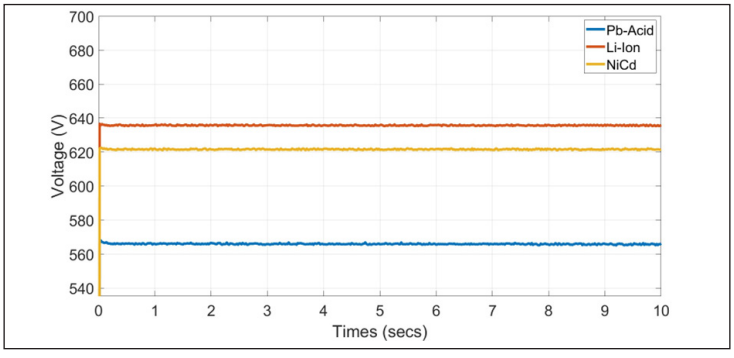

(b)

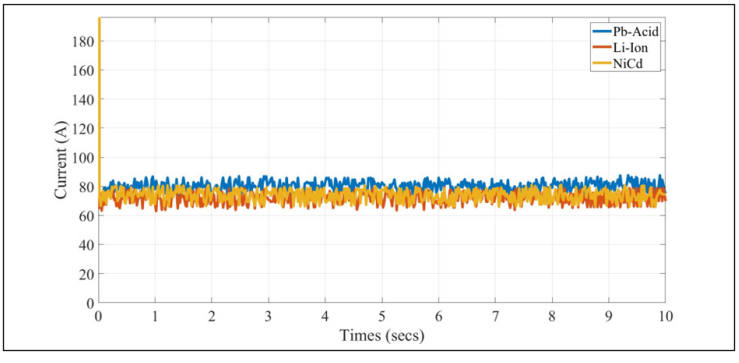

(c)

Figure 11. Result of battery Li-Ion, Pb-Acid, NiCD (a) SOC, (b) Voltage, (c) Current of different types of battery

Case 2 – Different Connection Arrangement of Battery

Figure 12 illustrates the SOC voltage and current for three battery configurations, series, parallel, and series-parallel, over time using a Li-Ion battery. All configurations show a decrease in SOC during discharge, with the series configuration (blue line) exhibiting the

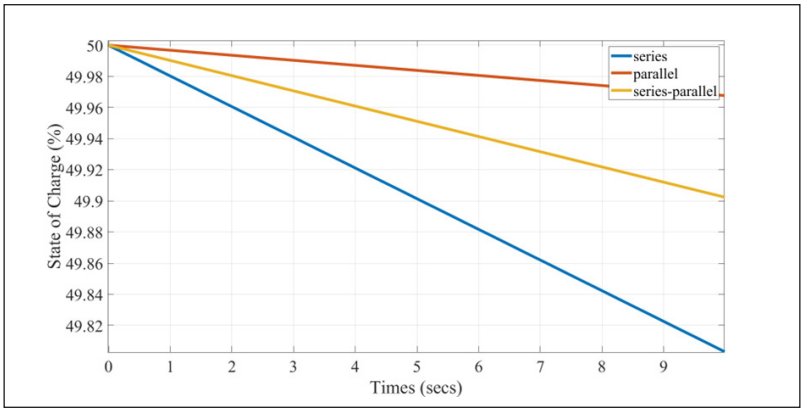

(a)

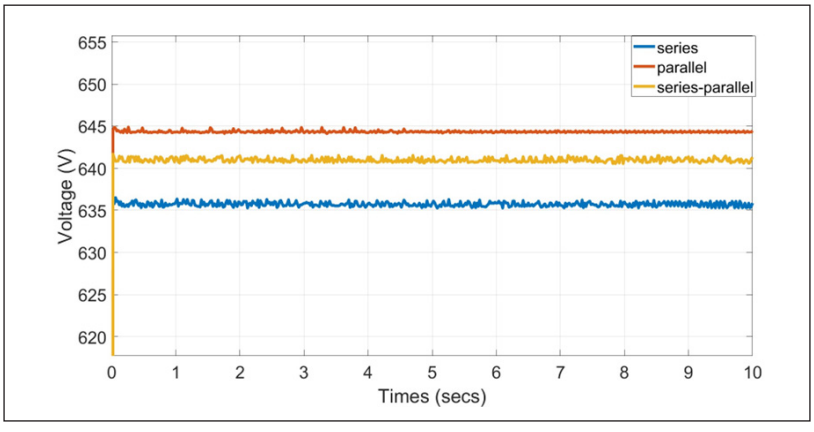

(b)

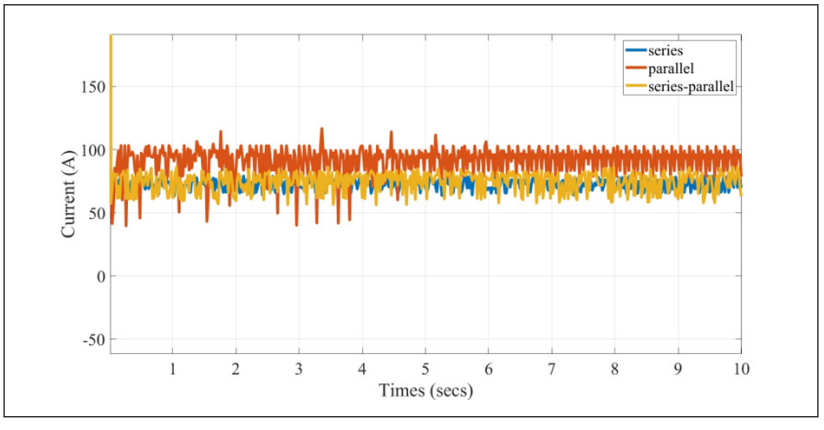

(c)

Figure 12. Result of battery connection (a) SOC, (b) Voltage, (c) Current of different battery arrangement

steepest slope, indicating the fastest discharge rate, dropping from 50% to about 49.82% by t=10 seconds. The parallel configuration (red line) shows a moderate discharge rate, decreasing to around 49.96%, while the series-parallel configuration (yellow line) maintains about 49.93% SOC, indicating the slowest discharge rate. Initially, all configurations start with a SOC of approximately 50%. As time progresses, the series configuration consumes energy more rapidly, while the series-parallel configuration retains charge most efficiently, making it suitable for applications requiring prolonged energy availability. The battery's SOC for series, parallel and series-parallel configurations dropped by 0.18%, 0.04%, and 0.07%, respectively. Voltage stability is observed across all configurations, with the parallel configuration having the highest nominal voltage, averaging around 645 V, followed by series-parallel at approximately 640 V and series at about 635 V. Minimal voltage fluctuations suggest reliable performance under load. Current fluctuations indicate varying load conditions, with the parallel configuration showing the highest and most variable current, averaging around 100 A, the series-parallel configuration averaging about 85 A with moderate fluctuations, and the series configuration having the lowest and most stable current, averaging around 70 A, indicating consistent performance under load. Overall, the series-parallel configuration demonstrates the best balance of discharge rate, voltage stability, and current consistency, making it ideal for applications requiring steady and prolonged energy output.

Case 3 – Battery Aging Factor

Figure 13 shows the SOC over time with and without the aging effect only for Li-Ion because the batteries exhibit more complex degradation mechanisms compared to Pb-Acid and NiCd batteries. Both lines decrease over time, as expected during battery discharge. The line with the aging effect (blue) has a steeper slope, indicating a faster discharge rate. In comparison, the line without the aging effect (orange) has a gentler slope, showing slower discharge and better efficiency. At the start (t=0), both configurations begin with a SOC of approximately 50%. By time t=10, the SOC with aging decreases to about 49.6%, whereas it remains higher at around 49.85% without aging. It was found that the SOC of a battery without aging decreased by 0.15% after 10 seconds, but the SOC of an aged battery decreased by 0.4%. This illustrates that the battery, without aging, retains its charge better, reflecting optimal performance. The graph highlights that aging leads to a faster SOC decline, emphasizing the importance of managing battery health. Additionally, the voltage with aging is slightly lower and exhibits moderate fluctuations, indicating increased internal resistance, while without aging, the voltage remains higher and more stable. The current with aging is lower overall and fluctuates slightly, whereas, without aging, the current is higher and more stable, reflecting better battery health and consistent current delivery under load. Overall, the battery without aging shows more stable performance across all metrics.

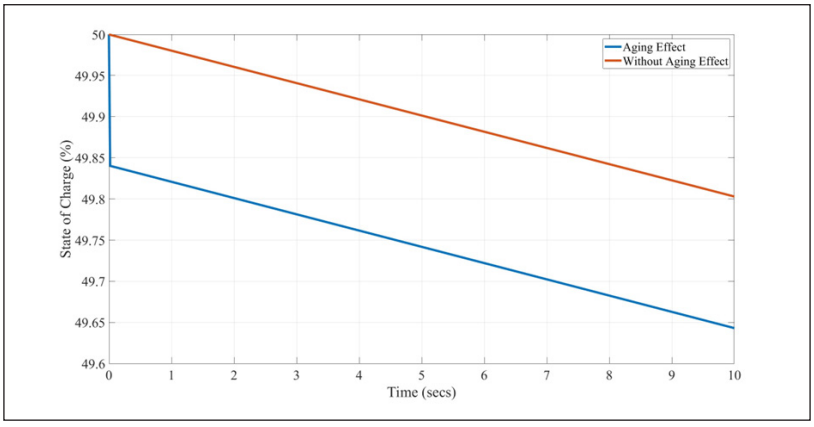

(a)

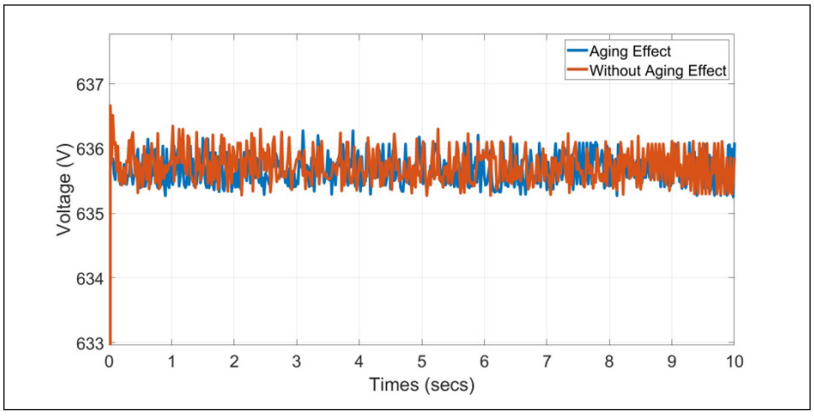

(b)

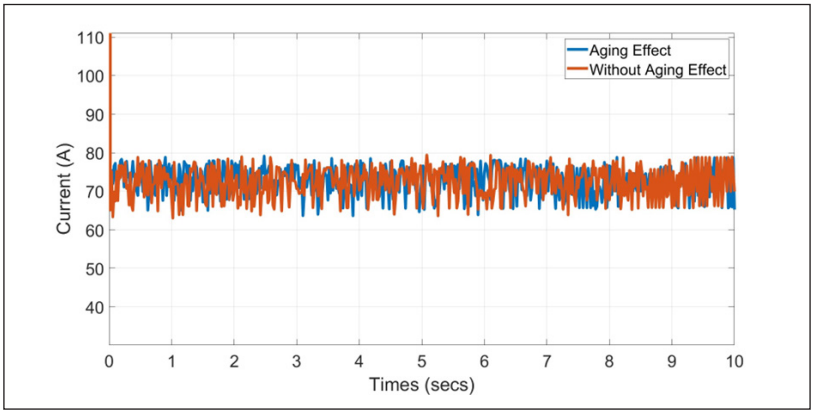

(c)

Figure 13. The result of the comparison of aging batteries and non-aging batteries is (a) SOC, (b) Voltage, and (c) Current for the aging factor of the battery

DISCUSSION

The study examines the performance of different battery types and configurations in various scenarios. Pb-Acid batteries discharge the fastest due to higher internal resistance, while Li-Ion batteries offer moderate discharge rates with better efficiency and energy density. NiCd batteries exhibit the slowest discharge, benefiting from robustness and low self-discharge rates. In terms of connection arrangements, the series configuration discharges rapidly, the parallel configuration maintains high voltage with variable current, and the series-parallel configuration provides a balance of efficient energy retention, stable voltage, and consistent current. Regarding the effects of aging, batteries without aging retain charge better, maintain more stable voltage and current, and underscore the importance of battery health management. Overall, Li-Ion batteries in a series-parallel configuration are ideal for ESS applications to charge EV batteries, offering a balance of efficiency, stability, and adaptability to varying load conditions. Figure 14 illustrates the charging of EVs by discharging ESS using selected battery properties and connections. The SOC graph shows the EV battery's charge increasing from 50% to approximately 50.6% by t=10 seconds, indicating efficient charging, while the ESS battery's SOC decreases slightly from 50% to about 49.9%, reflecting its role as the energy source. The voltage graph indicates that the ESS battery maintains a stable voltage of around 600 V, while the EV battery holds a steady voltage of about 450 V, suggesting consistent performance.

The current graph shows that the EV battery has a higher average current, around 100 A, with more fluctuations. In contrast, the ESS battery maintains a lower average current, around 75 A, with less variability. This demonstrates effective energy transfer, with the ESS supplying steady energy while the EV battery charges efficiently, highlighting the system's reliability and effectiveness. From Equations 2 and 3 charging and discharging, the EV battery can receive a current of 100 A, fully charging from 0% to 100% SOC in approximately 30 minutes. Meanwhile, the ESS will fully discharge its 100 Ah capacity with a discharging current of 75 A in about 1 hour and 33 minutes. This demonstrates that the ESS, with a constant current controlled by a PI controller to minimize losses, can act as a backup supply, supporting nearly three complete charges of the EV battery with good efficiency.

CONCLUSION

The simulation study successfully developed an EV charging system model using MATLAB. The analysis showed that Li-Ion batteries are most suitable for ESS due to their high energy density and stable voltage profile. The study also found that series-parallel battery connections enhance performance by 0.07%, offering balanced load distribution and improved maintenance. Additionally, the impact of battery aging was highlighted, emphasizing the need for effective battery management. As a result of the selected Li-Ion

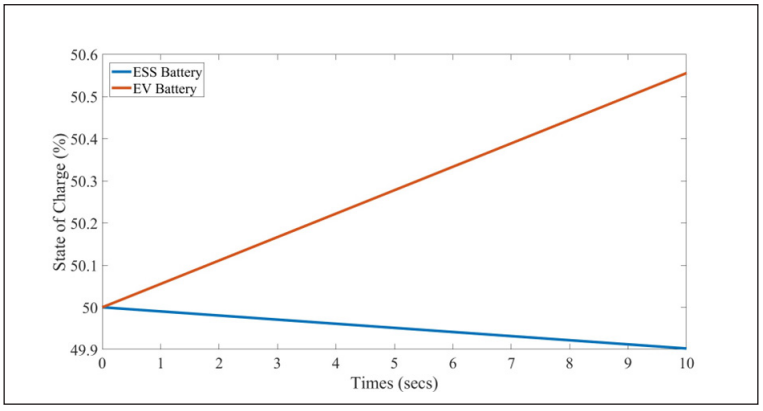

(a)

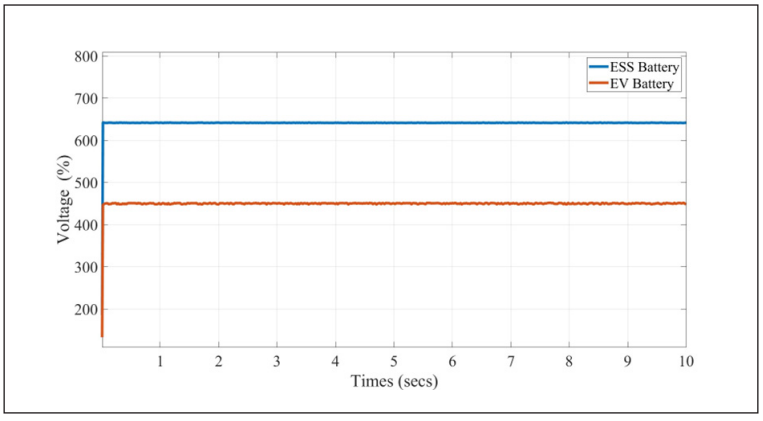

(b)

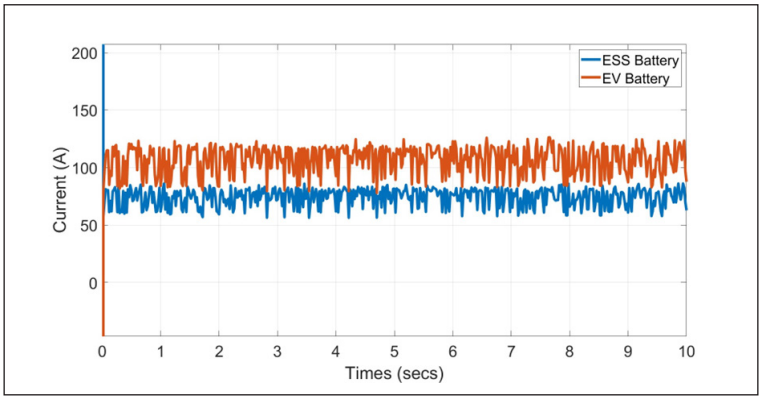

(c)

Figure 14. Graph of Charging EV by discharging ESS(a) SOC, (b) Voltage, (c) Current for best battery properties and connection arrangement

battery with no aging factor and series-parallel connection, the EV battery can receive a current of 100 A, fully charging from 0% to 100% SOC in approximately 30 minutes. Meanwhile, the ESS will fully discharge its 100 Ah capacity with a discharging current of 75 A in about 1 hour and 33 minutes. This demonstrates that the ESS, with a constant current controlled by a PI controller to minimize losses, can act as a backup supply, supporting nearly three complete charges of the EV battery with good efficiency. This research provides valuable insights into the automotive and renewable energy sectors, promoting more efficient and sustainable energy solutions. Future work should focus on advancements in battery technology and management systems to further optimize ESS and EV performance.

ACKNOWLEDGMENTS

The authors sincerely thank the individuals and organizations contributing to this research project. First, the authors would like to thank Petronas Research Sdn. Bhd. for their support. The authors also thank the CHAdeMO Association for their continuous technical support. Finally, the authors would like to thank the College of Engineering, Universiti Teknologi MARA, for the excellent facility provided for the research, administrative support, and technical assistance.

REFERENCES

Alghamdi, T. G., Said, D., & Mouftah, H. T. (2020). Decentralized game-theoretic approach for D-EVSE based on renewable energy in smart cities. In *ICC 2020-2020 IEEE International Conference on Communications (ICC)* (pp. 1-6). IEEE Publishing. https://doi.org/10.1109/ICC40277.2020.9148718

Al-Hanahi, B., Ahmad, I., Habibi, D., Pradhan, P., & Masoum, M. A. S. (2022). An optimal charging solution for commercial electric vehicles. *IEEE Access, 10*, 46162–46175. https://doi.org/10.1109/ACCESS.2022.3171048

Arfeen, Z. A., Khairuddin, A. B., Munir, A., Azam, M. K., Faisal, M., & Arif, M. S. B. (2020). En route of electric vehicles with the vehicle to grid technique in distribution networks: Status and technological review. *Energy Storage, 2*(2), Article e115. https://doi.org/10.1002/est2.115

Bais, A., Subhedar, D., & Panchal, S. (2024). Experimental investigations of a novel phase change material and nano-enhanced phase change material based passive battery thermal management system for Li-ion battery discharged at a high C rate. *Journal of Energy Storage, 103*, Article 114395. https://doi.org/10.1016/j.est.2024.114395

Cho, I., Lee, P. Y., & Kim, J. (2019). Analysis of the effect of the variable charging current control method on cycle life of li-ion batteries. *Energies, 12*(15), Article 3023. https://doi.org/10.3390/en12153023

Gong, X., Xiong, R., & Mi, C. C. (2015). Study of the characteristics of battery packs in electric vehicles with parallel-connected lithium-ion battery cells. *IEEE Transactions on Industry Applications, 51*(2), 1872–1879. https://doi.org/10.1109/TIA.2014.2345951

Hannan, M. A., Hoque, M. M., Hussain, A., Yusof, Y., & Ker, P. J. (2018). State-of-the-art and energy management system of lithium-ion batteries in electric vehicle applications: Issues and recommendations. *IEEE Access, 6*, 19362–19378. https://doi.org/10.1109/ACCESS.2018.2817655

Jeon, S. U., Park, J. W., Kang, B. K., & Lee, H. J. (2021). Study on battery charging strategy of electric vehicles considering battery capacity. *IEEE Access, 9*, 89757–89767. https://doi.org/10.1109/ACCESS.2021.3090763

Jiang, Q., Zhang, Y., Liu, Y., Xu, R., Zhu, J., & Wang, J. (2024). Structural optimization of serpentine channel water-cooled plate for lithium-ion battery modules based on multi-objective Bayesian optimization algorithm. *Journal of Energy Storage, 91*, Article 112136. https://doi.org/10.1016/j.est.2024.112136

Kumar, R. R., Bharatiraja, C., Udhayakumar, K., Devakirubakaran, S., Sekar, K. S., & Mihet-Popa, L. (2023). Advances in batteries, battery modeling, battery management system, battery thermal management, SOC, SOH, and charge/discharge characteristics in EV applications. *IEEE Access, 11*, 105761–105809. https://doi.org/10.1109/ACCESS.2023.3318121

Lehtola, T. A., & Zahedi, A. (2021). Electric vehicle battery cell cycle aging in vehicle to grid operations: A review. *IEEE Journal of Emerging and Selected Topics in Power Electronics, 9*(1), 423–437. https://doi.org/10.1109/JESTPE.2019.2959276

Li, S., Zhao, P., Gu, C., Li, J., Huo, D., & Cheng, S. (2023). Aging mitigation for battery energy storage system in electric vehicles. *IEEE Transactions on Smart Grid, 14*(3), 2152–2163. https://doi.org/10.1109/TSG.2022.3210041

Miao, Y., Hynan, P., Von Jouanne, A., & Yokochi, A. (2019). Current li-ion battery technologies in electric vehicles and opportunities for advancements. *Energies, 12*(6), 1–20. https://doi.org/10.3390/en12061074

Rosewater, D. M., Copp, D. A., Nguyen, T. A., Byrne, R. H., & Santoso, S. (2019). Battery energy storage models for optimal control. *IEEE Access, 7*, 178357–178391. https://doi.org/10.1109/ACCESS.2019.2957698

Said, D. (2021). Intelligent photovoltaic power forecasting methods for a sustainable electricity market of smart micro-grid. *IEEE Communications Magazine, 59*(7), 122-128. https://doi.org/10.1109/MCOM.001.2001140

Said, D., & Elloumi, M. (2022). A new false data injection detection protocol based machine learning for P2P energy transaction between CEVs. In *2022 IEEE International Conference on Electrical Sciences and Technologies in Maghreb (CISTEM)* (Vol. 4, pp. 1-5). IEEE Publishing. https://doi.org/10.1109/CISTEM55808.2022.10044067

Said, D., Cherkaoui S., & Khoukhi, L. (2015). Guidance model for EV charging service. In *2015 IEEE International Conference on Communications (ICC)* (pp. 5765-5770). IEEE Publishing. https://doi.org/10.1109/ICC.2015.7249241

Samadani, E., Panchal, S., & Mastali, M. (2012). *Battery Life Cycle Management for Plug-In Hybrid Electric Vehicle (Phevs) and Electric Vehicles (Evs)*. [Transport Canada Report]. University of Waterloo.

Schommer, A., Sciortino, D. D., Morrey, D., & Collier, G. (2024). Experimental investigation of power available in lithium-ion batteries. *Journal of Power Sources, 618*, Article 235168. https://doi.org/10.1016/j.jpowsour.2024.235168

Singh, A., Pal, K., & Vishwakarma, C. B. (2023). State of charge estimation techniques of Li-ion battery of electric vehicles. *E-Prime - Advances in Electrical Engineering, Electronics and Energy*, *6*, Article 100328. https://doi.org/10.1016/j.prime.2023.100328

Sundararajan, R. S., & Iqbal, M. T. (2021). Dynamic modelling of a solar energy system with vehicle to home and vehicle to grid option for newfoundland conditions. *European Journal of Electrical Engineering and Computer Science, 5*(3), 45-52. https://doi.org/10.24018/ejece.2021.5.3.329

Talele, V., Moralı, U., Khaboshan, H. N., Patil, M. S., Panchal, S., Fraser, R., & Fowler, M. (2024). Improving battery safety by utilizing composite phase change material to delay the occurrence of thermal runaway event. *International Communications in Heat and Mass Transfer, 155*, Article 107527. https://doi.org/10.1016/j.icheatmasstransfer.2024.107527

Timilsina, L., Badr, P. R., Hoang, P. H., Ozkan, G., Papari, B., & Edrington, C. S. (2023). Battery degradation in electric and hybrid electric vehicles: A survey study. *IEEE Access, 11*, 42431–42462. https://doi.org/10.1109/ACCESS.2023.3271287

Tran, M. K., DaCosta, A., Mevawalla, A., Panchal, S., & Fowler, M. (2021). Comparative study of equivalent circuit models performance in four common lithium-ion batteries: LFP, NMC, LMO, NCA. *Batteries, 7*(3), Article 51. https://doi.org/10.3390/batteries7030051

Umair, M., Hidayat, N. M., Ahmad, A. S., Ali, N. H. N., Mawardi, M. I. M., & Abdullah, E. (2024). A renewable approach to electric vehicle charging through solar energy storage. *PLoS ONE, 19*(2), Article e0297376. https://doi.org/10.1371/journal.pone.0297376